МЕТОДОЛОГИЯ МОРСКИХ ГИДРОФИЗИЧЕСКИХ ИССЛЕДОВАНИЙ

УДК 551.465

A.V.Babanin

Swinburne University of Technology, Melbourne, Australia

WIND INPUT, NONLINEAR INTERACTIONS AND WAVE BREAKING AT THE SPECTRUM TAIL OF WIND-GENERATED WAVES, TRANSITION FROM f^{-4} TO f^{-5} BEHAVIOUR

Behaviour of the equilibrium interval of the wave frequency spectrum is investigated. It is argued that spectra of Phillips, Toba and Zakharov-Filonenko are consistent with each other, and transition between f^{-4} and f^{-5} subintervals is parameterised by means of field data including those obtained at short fetches from Katsiveli research tower. Role of the wave breaking, wind input and nonlinear interactions in formation of the spectrum tail is discussed.

KEY WORDS: *Katsiveli tower, equilibrium interval, wave breaking, wind input, nonlinear interactions.*

Katsiveli research platform has been a site for long-term observations and dedicated field experiments over a period of 30 years, across a variety of oceanographic, meteorological and engineering applications. As far as the topic of wind-generated waves is concerned, value of the data obtained in Katsiveli are hard to overestimate.

In order to investigate evolution of wind waves, measurements along a large range of wave fetches are necessary. Surprising it may be, but it is the short fetches which are often missing in large-scale field experiments, and it is this gap which is covered by the observations from Katsiveli research tower in the Black Sea wind-wave data sets.

Because of the air-water density difference, waves develop slowly in response to the wind forcing. Depending on the wind, it takes tens or even hundreds of kilometres for the waves to grow mature and ultimately fully developed. Deployment of instrumentation all along such extended distances is not feasible, and even in field experiments now regarded classical the measurements were conducted either over only short fetches [1] or over only long fetches [2].

In order to achieve a desired variability of wave-development conditions in such circumstances, non-dimensional features of wave growth were employed following approach suggested by Kitaigorodskii in [3]. In short, within such approach the wave spectrum is presumed to remain self-similar in the course of its evolution, with the scaling property being an external parameter – wind speed. Thus, even for a constant dimensional fetch, non-dimensional fetches and other integral and spectral properties of the waves, scaled non-dimensional by means of the wind speed, can vary significantly depending on the wind.

There are, however, multiple issues with such wind-based scaling and respective dependences and parameterisations. First of all, since all the wave-growth properties are made dimensionless through the wind, the wind speed enters both sides of the dependences which fact leads to self-correlations [e.g. 4]. Second, strictly speaking, such normalisation is only applicable to so-called ideal conditions of wave development, i.e. waves forced by a constant offshore wind perpendicular to an infinitely-long coast. If these conditions are not satisfied, e.g. in case of slanting fetches, essential adjustments are needed to the wind speeds used for the scaling [e.g. 5].

What is the actual wind speed to be used for scaling is a big question in its own right. In the boundary layer near any interface, whether this is land or the ocean, the vertical profile of wind speeds is characterised by rapid velocity gradients. Customarily, it is the wind speed at 10m height above the surface which is employed because of convenience of the measurements. The measurements, however, are rarely done at the 10m precisely, and then they have to be converted into the U_{10} wind speeds by means of some boundary-layer models [see e.g. 6 – 9, among many others]. Such models are usually semi-empirical, with a great number of uncertainties [see e.g. 10 – 12 for a discussion and review]. Besides, the waves can be actually higher than 10m [e.g. 13, 14], and then the very concept of U_{10} becomes meaningless.

Also, lower parts of the boundary layer are affected by the wave-induced pressure/velocity fluctuations in the air which fact renders the wall-layer models unsuitable [e.g. 10, 15, 16]. Height of this lower sublayer depends on the length λ of surface waves and therefore, if it is to be avoided, there is no practical dimensional height for the characteristic wind in principle. Such height will depend on the scale of dominant waves, and argument has been made to use $U_{\lambda/2}$ wind speed rather than U_{10} [17 – 20]. As a result, multiple corrections, conversions and adjustments of the scaling parameter, which usually comes at some (often high) power, lead to many uncertainties and scatter in the respective non-dimensional analyses and their outcomes.

Moreover, and importantly, it is not the wind speed as such which drives the wave growth, it is the momentum flux τ from the wind to the waves which happens to have dimension of the wind speed squared:

$$\tau = \rho_a u_*^2 = \rho_a C_d U_{10}^2 \,. \qquad (1)$$

Here, ρ_a is air density, and u_* is so-called friction velocity, i.e. some fictitious velocity which signifies the flux. In order to obtain u_* directly, either the momentum flux or the logarithmic boundary-layer wind profile have to be measured [e.g. 9, 11]. In absence of such measurements which is usually the case, it can be obtained from the wind speed U_{10} by applying drag coefficient C_d as depicted in (1).

Thus, as far as the wind scaling of wave growth is concerned, it is u_* rather than anything else which should be used as a characteristic velocity. Here, however, C_d is another problem. The drag coefficient is a purely empirical quantity and is effectively intended as a proxy for the structure of the boundary layer, i.e. it is meant as a means to convert wind measurements at some height into the momentum flux at the ocean surface. Such proxy cannot be anything but a poor surrogate as the boundary layer physics, even to a non-specialist in this particular area, clearly cannot be replaced by a single number or even by a dependence of this number on one, two or a few relevant parameters. In [11], fifteen properties and phenomena which can influence the drag coefficient are listed, plus the entire suit of additional characteristics at hurricane-like winds, and here we can also add the sea surface temperature to this set, following [21]. Among these properties, effects due to temperature stratification [22, 23], presence of swell [24, 25], gustiness and unsteadiness of the wind [11, 26], directional spread in the wave system [27], can change the drag coefficient by a factor of two or more. As a result, empirical parameterisations of the drag coefficient are characterised by an enormous scatter which has not improved over some 30 – 40 years in spite of all the recent technological, computing, and data logging and collection advances. This scatter then feeds back into the scaling problem for non-dimensional wave-growth approach.

For the offshore winds, which are the element of ideal-development conditions as mentioned above, many more problems arise. Structure of the boundary layer is transitional when the air flow crosses from land to the sea. That is, in a way, the wind for some time 'remembers' roughness over the land while already moving over the sea, and even though the near-interface wind immediately adjusts itself to the new surface, U_{10} may still indicate the roughness values of land upstream for some time. This fact is bound to have a major impact on models of wave development at short fetches as no characteristic U_{10} wind speed can be specified in such case [e.g. 28]. Even at steady meteorological circumstances, mean wind speed at a reference height changes as the wind propagates away from the coast [29].

Thus, non-dimensional dependences of the wave growth in terms of the wind speed are prone to self-correlations, large scatter and a variety of inconsistencies. In [30], twenty three such dependences, accumulated over some 50 years of field experiments and campaigns, were scrutinised, and only four of them were selected as plausible in physical terms. The Black Sea data set, obtained from observational platforms at sea including the Katsiveli research tower, was recognised the best among the four.

Before describing this data set, another issue has to be outlined, which delivered a major blow to the 50-year old tradition of studying the wave evolution by means of the dimensional scaling in terms of an external property, i.e. the wind speed. In [30], it was argued that the non-dimensional features of self-similar wave growth have to be scaled by internal wave-field properties, that is fluxes of energy, momentum or wave action.

In [31], this idea was further elaborated. It was shown that at different stages of the wave development, the wave spectrum is shaped due to qualitatively different balances between the energy source terms in the wind-wave system. At the initial stage, the self-similar wave-spectrum evolution is driven in conditions of constant momentum flux. Such kind of development is described by Hasselmann law [32] of

$$H \sim T^{5/3}, \tag{2}$$

where H is characteristic wave height and T is characteristic wave period. The growing sea is described by the Toba law [33]

$$H \sim T^{3/2}, \tag{3}$$

the best-known because such conditions occur most frequently. Mature waves are characterised by Zakharov-Zaslavskii law [34]

$$H \sim T^{4/3}. \tag{4}$$

These differences imply different dynamics and physics in the course of wave growth and yet, if comprehensively proved, are impossible to see by means of the traditional wind-scaling approach.

The Black Sea data set. Such long Introduction was necessary in order to explain the importance and uniqueness of the Black Sea data set of the wind-wave growth and evolution which includes measurements and observation obtained at the Katsiveli platform. Measurements at a single location, which then rely on the non-dimensional scaling, suffer from shortcoming at the very least, and potentially from major disadvantages as discussed above.

Of these, wind-wave observational field campaign at the research tower in Lake Ontario [5] is recognised as one of the best because, apart from many other merits, while measurements were conducted at a single point in this experiment in the large enclosed lake, different dimensional fetches were actually available depending on direction of wave propagation. What is of principal significance, both waves at short fetches (the shortest onshore distance was 1km) and long fetches (~300 km) were recorded. Wave-growth dependences for the short and long fetches are essentially different, and wind-based scaling cannot pick these differences up. Therefore, even results of such famous field experiment as JONSWAP [2] had to be corrected by adding laboratory points to the data pool, and the laboratory substantially corrupted the outcomes [see e.g. 8, 30, 35]. Similarly, observations in Hakata Bay [1] which set standards in this field for many years to come, but were conducted at a short-fetch site, were clearly inapplicable to the open-sea waves. As a result, in [30] both these classical experiments were placed in the worst-performing group (no.4) when their dependences were subjected to strict physical tests. The Lake Ontario parameterisations, although allowing for varying fetches, but still carried out in a single point and relied on wind scaling, were ranked into group 2 in [30].

In this regard, the Black Sea data were regarded the best in group 1. The experimental approach was different at the Air-Sea Interaction Department of the Marine Hydrophysical Institute (MHI) where the wind-wave field observations in the 80 s and early 90 s were conducted from different platforms which allowed for multiple choices of dimensional and non-dimensional wave fetches. Locations of the platforms are shown in Fig.1.

The open-sea observational site was at an oil rig at the North-Western shelf of the Black Sea, with the deep-water wave fetches ranging from some 30 km for the easterly winds through 50 – 70 km from the north and up to 150 km for the westerlies. In the southern direction the fetch was infinite, limited by the size of meteorological formations rather than by the distance to the shore.

Open-sea long-fetch observations are quite common and there are many, as summarised in [30]. What made the Black Sea data set collected by MHI unique and high-quality was the data obtained at short fetches from the Katsiveli research tower. Location of this platform is indicated in Fig.1 and detailed in Fig.2.

In geographical terms, Fig.2 is reversed, i.e. North is approximately facing down and East is to the left (see Fig.1 for the geographically correct position of the

F i g . 1 . Location of research towers in the Black Sea (pluses). Figure is reproduced from [8], copyright of the American Meteorological Society.

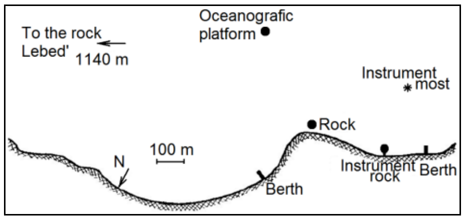

F i g . 2 . Position of the near-shore research tower in Katsiveli. Figure is reproduced from [8], copyright of the American Meteorological Society.

coastline). Deep-water initial-stage wave fetches at this site, depending on the wind direction, varied from 600 m to 1 km. It is these short-fetch data points which made the Black Sea data set distinctly unique, and highlighted features that proved difficult to reveal in many other field experiments as will be further described below.

Over the years, these Black Sea data, with the crucially important Katsiveli subset, were used to study integral [10, 30, 36, 37], spectral [10, 37] and directional properties [37 – 39] of the wave growth, wind-wave-current interactions [40], non-linear effects in the wave field [37, 41, 42], wave-group and bandwidth properties [10, 36, 37, 43], wave breaking and dissipation [12, 44 – 48]. Thus, the impact of the Black Sea field campaign on the wind-wave studies is essential across the entire spectrum of relevant topics and applications. In this article, we will concentrate on a new issue, which will be attended with use of the Katsiveli data, that is the physics at the small-scale end of the wave system.

Role of the input and redistribution energy fluxes, and wave breaking in maintaining the level of the spectrum tail. Formulations for the high-frequency tail of the wave spectrum which describes the small-scale end of the wave system does not explicitly depend on a formulation for the spectral peak. Here, we will refer to the JONSWAP spectral shape as a matter of convenience, since it the most broadly employed parameterisation – in order to have a reference to define what is meant as the level of this tail. The JONSWAP spectrum, which is a result of averaging frequency-spectrum shape $F(f)$ observed in ideal fetch-limited conditions, was suggested as an outcome of the field campaign conducted in the North Sea [2]:

$$F(f)=\alpha g^2(2\pi)^{-4} f^{-5}\exp\left(-\frac{5}{4}\left(f/f_p\right)^{-4}\right)\gamma^{\exp\frac{\left(f-f_p\right)^2}{2\sigma^2 f_p^2}} . \qquad (5)$$

Here, f is frequency, f_p is peak frequency, g is gravitational acceleration, γ and σ are parameters of the spectral-peak shape. The *exponent* in this parameterisation was introduced much earlier by Pierson and Moscowitz for the fully developed spectrum in [6] as a means to allow the front face of the spectrum to curve down, i.e. to have the peak as such, and the actual contribution of JONSWAP is the γ-expression which defined enhancement and shape of the peak of the waves that are still developing. These details are not relevant here and we refer the reader to [2, 5, 8] for them if necessary.

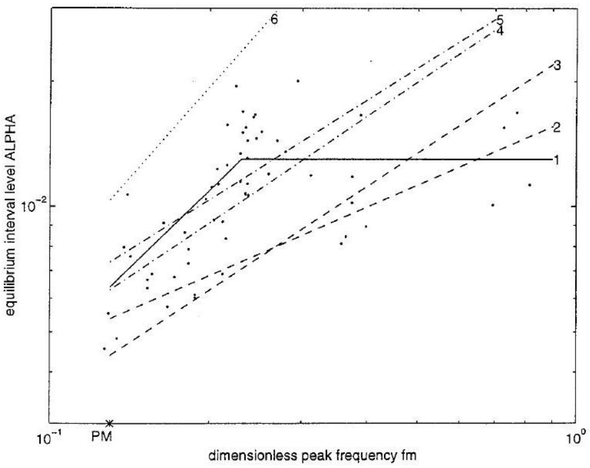

Fig.3. Dependence of spectrum-tail level α from (5) on dimensionless frequency $\tilde{f}_m$ (6). Data points and the solid line 1 (7) signify the Black Sea measurements and dependence. Other lines are parameterisations from [5] (line 2), [49] (line 3), [50] (line 4), [2] with laboratory data (line 5) and without (line 6). *PM* at the bottom axis indicate the full development stage according to [6]. Figure is reproduced from [8], © American Meteorological Society.

What is relevant for us, is the first part of expression (5). Here, f^{-5} is the asymptotic behaviour of the JONSWAP spectrum, and α determines the level of the entire spectrum including of course the level of the asymptotic tail.

Dependence of α on dimensionless frequency $\tilde{f}_m$ is shown in Fig.3, reproduced from [8]. In terms of notation of the present paper, the dimensionless frequency is

$$\tilde{f}_m = \tilde{f}_p = \frac{U_{10} f_p}{g} = \frac{1}{2\pi}\frac{U_{10}}{c_p}, \qquad (6)$$

where c_p is phase speed of waves at the spectral peak, i.e. those with frequency f_p. Ratio U_{10}/c_p signifies strength of the wind forcing: for young and slow waves $U_{10} >> c_p$ and the forcing is strong. As the waves develop, downshifting progresses and peak waves move faster, the forcing goes down until it disappears at $U_{10} \approx c_p$.

In Fig.3, the data points and the segmented solid line indicate the Black Sea measurements and parameterisation. A number of other parameterisations, also based on field data, are shown as specified in the Figure's caption. All the dependences, other than that of the Black Sea, are based on large-fetch data and, if extrapolated to higher values of $\tilde{f}_m$ they predict unlimited growth of the equilibrium level α. According to [8], this is not the case.

The difference is due to the Katsiveli data points on the right, i.e. those for young waves with high values of wind forcing and dimensionless peak frequency. Clearly these points indicate that, if one has measurements at short fetches, one cannot keep extrapolating the growth observed at longer fetches. For younger waves (which in case of the ideal fetch-limited development means short fetches) the equilibrium level stays approximately constant, and it is only at some mature wave ages that it starts to respond to the weakening wind forcing and to decrease towards the Pierson-Moscowitz magnitude (note that wave development progresses from right to left). Similar two-phase behaviour is also consistent with behaviour of the spectral bandwidth, and in [8] it was parameterised as

$$\alpha = \begin{cases} 8{,}03 \cdot 10^{-2}\, \tilde{f}_p^{1{,}24} & \text{for} \quad \tilde{f}_p \le 1{,}23, \\ 13{,}2 \cdot 10^{-3} & \text{for} \quad \tilde{f}_p > 1{,}23. \end{cases} \qquad (7)$$

Thus, the equilibrium level of the wave frequency spectrum, even though with some variations, remains remarkably stable given the very large magnitudes of differences in wind forcing. These differences occur both in absolute values, that is in terms of the wind speed which in the Black Sea measurements varied from near-zero to some 30 m/s, and in relative terms across the wind-wave scales, that is if $U_{10}/c_p = 1$ for waves with f_p = 0,1 Hz, then at the 2 Hz tail end it will be $U_{10}/c_p \sim 40$ (neglecting the surface-tension contribution for clarity).

The first analytical justification for the equilibrium range of the spectrum, based on dimensional argument, was proposed by Phillips in [51]. The idea of the equilibrium spectrum tail was already in the air, and a number of experimentalists had suggested their dependences for such spectral interval. The first parameterisation was by [52] for a ‘fully-developed spectrum’,

$$F(\omega) = C\omega^{-6} \exp\left(\frac{-2g^2}{\omega^2 U^2}\right), \tag{8}$$

where $\omega = 2\pi f$ is radian frequency, $C = 1{,}4\cdot 10^3$ cm/s^3 is a dimensional constant and U is some estimate of the wind speed. Parameterisation of [53] was measured in the range of wave fetches X = 400 – 1350 m and wind speeds U_{10} = 5 – 8 m/s and stated the fact that, even though the spectra themselves were clearly developing, with the spectrum peak and the total energy evolving, the tails “obtained in different conditions very nearly coincide and become apparently independent of the fetch and of the strength of the wind”:

$$F(\omega) = 7{,}0\cdot 10^3 \omega^{-5}. \tag{9}$$

[54] produced a parameterisation which is already remarkably familiar (see (5)):

$$F(\omega) = \alpha g^2 \omega^{-5} \exp\left(-0{,}657\frac{2\pi}{T\omega^4}\right), \tag{10}$$

where T is “a ‘mean wave period’ which depends upon wind speed and the state of development of the sea”. [54] found that constant $\alpha = 7{,}4\cdot 10^{-3}$, obtained from observations in [53], was consistent with his spectra.

In [51], it was rightly argued that for the spectrum parameterisation to be physically sound, its dimension has to be correct. Phillips produced a rather long list of physical dimensions to be considered, i.e. air and water densities ρ_a and ρ_w, friction velocity u_*, surface roughness length z_0, acceleration g, water surface tension σ (not to be confused with the σ from (5)) and viscosity ν, together with the relevant spectral scales k (wavenumber) and ω.

In different parts of the spectrum, different combinations of the dimensional properties may be valid and/or significant, but when it comes to the gravitational range of surface waves, it was u_* which represented the wind stress in (1) and gravitational acceleration g that remained. If talking about the spectrum tail, which clearly exhibited some level of saturation in the spectra of [53], [51] argued that this saturation signifies some limiting shape of the wave crests which is apparently due to the waves breaking and not being able to grow any further.

With respect to the breaking, [51] argued that “the geometry of the limiting shape near the sharp crests is determined by the condition that the downward acceleration should not exceed g, so that the asymptotic forms... would not be expected to involve u_*. An increase in u_*... should not influence the geometry of such a sharp crest itself". [51] even made a footnote remark that "we have excluded a different possible type of surface instability in which the sharp crests may be 'blown off' by very high winds".

We must notice that this is exactly the view of the breaking onset that we have these days [12, 55, 56]. As discussed in detail in papers [55, 56] and review [12], the breaking onset is defined by the limiting steepness

$$\frac{Hk}{2} \approx 0{,}44\,, \tag{11}$$

and it is only at extreme conditions that the wind can reduce this steepness, and even then only marginally.

If so, the original argument of [51] is right and the only relevant dimensional parameter for this part of spectrum is g. This led to the frequency spectrum of the saturated interval

$$F(\omega) = \alpha g^2 \omega^{-5} \tag{12}$$

and wavenumber spectrum

$$F(\mathbf{k}) = \alpha_k(\theta) k^{-4}\,. \tag{13}$$

Following (9), [51] defined his constant as α = 7,4·10^{-3}. Expression (13) determines spectral densities in different directions of wavenumber vector **k**, and the dimensionless coefficient α_k depends on this direction θ.

Parameterisations (12) – (13) must have been the first physical and even quantitative account for the wave-breaking effects on behaviour of the wave system. By limiting the growth of waves, they define the shape of the spectrum tail and even set its level.

Many more measurements of the equilibrium interval have been conducted since 1958. The level α proved to be not that constant (see [8], Fig.3 and eq.(7) above). The early observations of [53] were conducted at what we would now classify as relatively light winds, and for stronger winds even Phillips himself reconsidered this value [57].

According to (7), the tail level α responds to the wind forcing if $U_{10}/c_p < 1{,}45$. At such forcing, apparently, the average Phillips' 'geometry of the limiting shape' of the wave crests can change due to, perhaps, changing rates of the breaking occurrence in the high-frequency spectral bands.

Once it reaches, however, α = 13,2·10^{-3} at $U_{10}/c_p \geq 1{,}45$, level of the f^{-5} tail does not grow up further on average even if the wind forcing increases very significantly (Fig.3). As shown in [12, 58, 59], such situation does not actually mean that the breaking rates of short waves reached 100 %, they stay essentially below this ultimate percentage. Therefore, this condition can only signify a change of the breaking severity. Thus, for the younger waves, the breaking reacts to the changing wind forcing by altering the dissipation rates rather than the rate of breaking occurrence, in its role of maintaining the spectrum-tail level.

At the hurricane-like winds, that is for very young waves, with 100 % breaking rate of the short waves indeed occurring, the tail is still roughly at the same level range (unpublished). This fact further highlights the significant role of the breaking in formation of the wave spectrum as we know it. In such case, the forcing is most extreme, but the spectrum level only changed by less than a factor of 2. That is, the wave-breaking control still maintains approximately the same tail shape and balances the much grown wind input by adjusting its severity up: i.e. the extra wind input is lost locally to the dissipation, but the spectrum tail more or less holds its level.

While talking about the saturation level, it must be mentioned of course that using the same dimensional argument as [51], but assuming the role of the wind still essential, Toba in [60] obtained a different parameterisation for the spectrum tail:

$$F(\omega) = \beta u g \omega^{-4}, \tag{14}$$

i.e. he argued in favour of a quasi-equilibrium interval, whose level depends on some characteristic wind speed u, in addition to the gravitational acceleration g. Well before that, Zakharov and Filonenko in [61] achieved exact analytical solution of the Hasselmann equation for the spectrum defined by interactions in the system of nonlinear waves, which also produced an ω^{-4} tail:

$$F(\omega) = c_K p^{1/3} g \omega^{-4}. \tag{15}$$

Here, the spectral level varies as a function of energy flux p across the spectrum, and c_K is Kolmogorov constant.

The observations were divided and produced both f^{-5} and f^{-4} parameterisations, e.g. JONSWAP spectrum [2] and the Donelan-Hamilton-Hui spectrum [5], respectively. The f^{-4} interval required more attention as the initial formulations (14) and (15) seemed contradictory: the first one associated the equilibrium with the external wind forcing and the second one with the internal nonlinear flux. The contradiction was basically resolved by [62] who concluded, based on a comprehensive collection of field data sets, that

$$u = (U_{10}^2 c_p)^{1/3} - u_o, \tag{16}$$

where the first term on the right defines the external energy flux. This flux can now be related to the internal flux p, and the contradiction is answered. u_0 here is a dimensional offset of the experimental dependences, which complicates the theoretical argument, but is apparently the robust feature of the experimental analysis by [62].

In the meantime, based on experimental evidence and theoretical argument, there came understanding that both f^{-4} and f^{-5} subintervals are present at the tail, the first one being closer to the peak [4, 39, 49, 62, 63]. Moreover, it became clear that the total wind input, integrated over entire spectrum $F(f)$ cannot converge to the total wind stress known independently, unless f^{-5} subinterval does exist [64, 65]. For the oceanic waves, the transition was observed at frequency $\omega_t \approx 2{,}5 - 3$ of the peak frequency [49, 63]. In [4], based on 'grand average' of many measurements of the saturation spectra from different data sets, a dimensional value for such frequency was indicated as

$$\omega_t \approx 5 \frac{g}{U_{10}}, \tag{17}$$

which can alternatively be expressed as

$$\tilde{\omega}_t = 2\pi \tilde{f}_t = \frac{U_{10}}{c_p} \approx 5. \tag{18}$$

Now, with the view of (16) above, the transition frequency can be parameterised in terms of the peak frequency and characteristic wind speed. Eqs. (12), (14) and (16) can now be combined to give a dependence of the transitional frequency on peak frequency and wind speed:

$$\omega_t = \frac{\alpha}{\beta}\frac{g}{u} = \frac{\alpha}{\beta}\frac{u}{(U_{10}^2 g/\omega_p)^{1/3} - u_o}. \qquad (19)$$

α can be defined by (7), and $\beta = 6{,}09\cdot 10^{-3}$ according to [62].

In Figure 4, ratio ω_t/ω_p is plotted versus dimensional peak frequency f_p (top panel) and versus the wind forcing U_{10}/c_p in the bottom panel. Range of changes of the latter corresponds to the peak frequencies of the top subplot, and the wind speeds shown are U_{10} = 10, 15, 20, 30 and 40 m/s (top to bottom).

At typical oceanic winds of U_{10} ~ 10 m/s and typical wave age U_{10}/c_p ~ 1,2, (19) produces the transition at $\omega_t \approx 2{,}2\omega_p$ which is close, even though slightly below the values of [49, 63] mentioned above. If dependence (17) is used, then for U_{10} ~ 10 m/s and $\omega_t \approx 2{,}2\omega_p$ it gives f_p = 0,35 Hz which is exactly what the corresponding line in the top subplot of Fig.4 indicates.

The highest transitional frequency ω_t, for individual cases over the five wind speeds, is in the range of $\omega_t \approx 1{,}8 - 2{,}7\omega_p$. The lowest transitional frequency is an asymptotic hypothetical value below the peak ($\omega_t < \omega_p$) which basically means that in those circumstances the f^{-5} interval will extend all the way to the spectral peak, i.e. there will be no f^{-4} subinterval.

Such condition (i.e. no f^{-4} subinterval) is never reached for wind speeds U_{10} = 10 m/s (top subplot), that is at such wind the spectrum will always have the two subintervals. At all the other wind speeds, for wind forcing stronger than $U_{10}/c_p \approx$ 3,9 – 7,2, there will be only f^{-5} spectrum tail, and therefore no condition where the spectrum shape is controlled by the nonlinear fluxes (15) will take place.

In accord with (7), maximal transitional frequency ω_t will occur at

$$U_{10}/c_p \approx 1{,}45. \qquad (20)$$

Both for the younger waves and more mature waves, it draws closer to the peak. This demonstrates the relative significance of the breaking and of the nonlinear fluxes in formation of the spectrum at the respective wave-development stages.

In this regard, it can be expected that the f^{-5} tail comes closer to the peak at strong wind forcing, and the f^{-4} tail may even eventually disappear at such forcing. The fact that this is also a trend when the waves are maturing towards full development at U_{10}/c_p less than (20), however, is somewhat counter-intuitive.

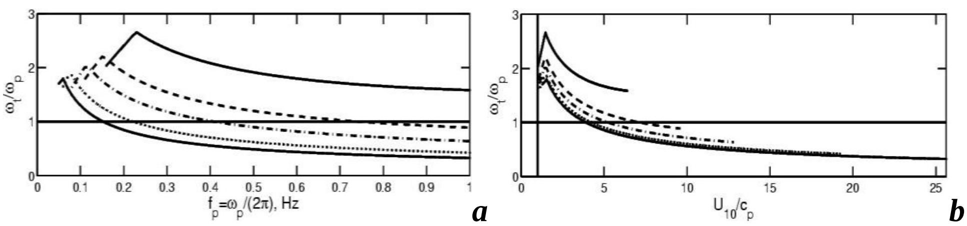

F i g . 4 . In both panels, top to bottom wind speeds are U_{10} = 10, 15, 20, 30 and 40 m/s. Ratio of transitional and peak frequencies ω_t/ω_p versus peak frequency $f_p = \omega_p/(2\pi)$ (a) and versus wind forcing parameter U_{10}/c_p (b).

This is, apparently, due to the reduction of α in (12). Such reduction, however, is a consistent feature of the observations, not only of the parameterisation (7) by [8], but also of those by [2, 5, 49, 50]. Moreover, (20) corresponds exactly to the transition of the regime of α behaviour in the dependence (7) of [8].

Discussion and conclusions. How can the result of Section III be explained in terms of the competition between the wave-breaking and the weak-turbulence mechanisms for the control over the saturation interval? At this stage we can only offer a tentative reasoning rather than an explanation based on direct experimental facts or theoretical grounds.

First of all, even if it may seem so, the competition is not between the external wind forcing and nonlinear internal fluxes, it is between the breaking/dissipation and such fluxes. Even though the forcing is large at the upper end of the equilibrium interval in Fig.4, the wind does not make the waves break directly, except in a hurricane-like conditions. Breaking happens either due to hydrodynamic reasons, i.e. wave superposition or modulational instability [55, 56, 66], or is induced [58, 67, see also 12 for discussions].

For the spectrum tail, the induced breaking, due to various influences of the large waves, dominates (see [12]). The transition between prevalence of induced breaking over the inherent breaking happens at approximately the same relative frequency $\omega_t \sim 3\omega_p$ (Filipot, 2010, private communication) as the transition ω_t in this article. This means that most of the breaking which we see to control the f^{-5} interval is induced, and whatever the wind does to stimulate this breaking is done mostly indirectly through altering the long-wave conditions in the field.

On the other hand, this induced breaking for younger waves reacts to the changing wind-forcing conditions by adjusting the breaking strength, whereas the breaking rates as such do not necessarily change (see also [59]). This is for $U_{10}/c_p > 1{,}45$. For the mature waves of $U_{10}/c_p < 1{,}45$, as was already discussed in this article, the induced breaking is likely to simply alter the rate of occurrence because of the wave age.

Why and how the dominant waves do that to the induced breaking of the short waves is yet to be understood, but one way or another, at both sides of the $U_{10}/c_p \approx 1{,}45$ wave age, the extent of the f^{-4} interval starts shrinking. This shortening leads to complete disappearing of this dynamic spectral range for younger waves, but for the mature waves such interval controlled by the nonlinear fluxes always exists. Even at full development, $\omega_t = 1{,}6 - 2{,}1\omega_p$ depending on the wind speed (Fig.4, *b*). Transitional frequency $1{,}6\omega_p$, however, which occurs at full development at wind speed $U_{10} = 40$ m/s is very close to the spectral peak whose half-width is approximately $1{,}3 - 1{,}5\omega_p$. Therefore, at very strong winds, width of the f^{-4} interval, even when it exists, is quite short.

To conclude this article, we would also briefly mention that wave breaking can make other, perhaps even somewhat unexpected contributions to the spectrum tail. [68], for example, showed by means of the deterministic modelling of directional waves that power of the dissipation function, if altered, influences the asymptotic wave tail. Breaking of large waves can actually generate short waves and ripples [e.g. 69, 70]. Such contribution is interesting, but is perhaps small and is yet to be quantified. Control of the level of the f^{-5} interval, which is achieved both through the breaking frequency and strength, and its competition with the nonlinear fluxes for the shape of the spectrum tail, is, however, a very important role of the breaking in wave fields with continuous spectrum.

REFERENCES

1. *Mitsuyasu H., Nakamura R., Komori T.* Observations of the wind and waves in Hakata Bay // Rep. Res. Inst. Appl. Mech. Kyushu University.– 1971.– 19.– P.37-74.
2. *Hasselmann K., Barnett T.P., Bouws E., Carlson H., Cartwright D.E., Enke K., Ewing J.A., Gienapp H., Hasselmann D.E., Kruseman P., Meerburg A., Muller P., Olbers D.J., Richter K., Sell W., Walden H.* Measurements of wind-wave growth and swell decay during the Joint North Sea Wave Project (JONSWAP) // Dtsch. Hydrogh. Z. Suppl.– 1973.– A8(12).– P.1-95.
3. *Kitaigorodskii S.A.* Applications of the theory of similarity to the analysis of wind-generated wave motion as a stochastic process // Bull. Acad. Sci. USSR, Geophys. Ser., Engl. Transl.– 1962.– 1.– P.105-117.
4. *Kahma K.K., Calkoen C.J.* Reconciling discrepancies in the observed growth of wind-generated waves // J. Phys. Oceanogr.– 1992.– 22.– P.1389-1405.
5. *Donelan M.A., Hamilton J., Hui W.H.* Directional spectra of wind-generated waves // Phil. Trans. R. Soc. Lond.– 1985.– A315.– P.509-562.
6. *Pierson W.J. Jr., Moskowitz L.* A proposed spectral form for fully developed wind seas based on the similaruty theory of S.A. Kitaigordskii // J. Geophys. Res.– 1964.– 69.– P.5181-5190.
7. *Snyder R.L., Dobson F.W., Elliott J.A., Long R.B.* Array measurements of atmospheric pressure fluctuations above surface gravity waves // J. Fluid Mech.– 1981.– 102.– P.1-59.
8. *Babanin A.V., Soloviev Y.P.* Field investigation of transformation of the wind wave frequency spectrum with fetch and the stage of development // J. Phys. Oceanogr.– 1998.– 28.– P.563-576.
9. *Young I.R., Banner M.L., Donelan M.A., Babanin A.V., Melville W.K., Veron F., McCormic C.* An integrated study of the wind wave source term balance in finite depth water // J. Atmos. Oceanic Tech.– 2005.– 22.– P.814-828.
10. *Chalikov D., Belevich M.* One-dimensional theory of the wave boundary layer // Boundary-Layer Meteorol.– 1993.– 63.– P.65-96.
11. *Babanin A.V., Makin V.K.* Effects of wind trend and gustiness on the sea drag: Lake George study // J. Geophys. Res.– 2008.– C113.– C02015, doi:10.1029/2007JC004233.– 18 p.
12. *Babanin A.V.* Breaking of ocean surface waves // Acta Physica Slovaca.– 2009.– 59.– P.305-535
13. *Greenslade D.J.M.* A wave modelling study of the 1998 Sydney to Hobart yacht race // Aust. Met. Mag.– 2001.– 50.– P.53-63.
14. *Liu P.C., Chen H.S., Doong D.-J., Kao C.C., Hsu Y.-J.G.* Monstrous ocean waves during typhoon Krosa // Ann. Geophysicae.– 2007.– 26.– P.1327-1329.
15. *Kudryavtsev V.N., Makin V.K., Meirink J.F.* Simplified model of the air flow above the waves // Boundary-Layer Meteorol.– 2001.– 98.– P.155-171.
16. *Chalikov D., Rainchik S.* Coupled numerical modelling of wind and waves and theory of the wave boundary layer // Boundary-Layer Meteorol.– 2010. (*in press*)
17. *Chalikov D., Sheinin D.* Direct modeling of one-dimensional nonlinear potential waves / Ed. By W.Perrie. Nonlinear Ocean Waves (Adv. in Fluid Mechanics).– 1998.– 17.– P.207-258.

18. *Donelan M.A.* Wind-induced growth and attenuation of laboratory waves / Eds. By S.G.Sajadi, N.H.Thomas, J.C.R.Hunt. Wind-over-Wave Couplings. Perspective and Prospects.– Clarendon Press, Oxford, 1999.– P.183-194.
19. *Chalikov D., Sheinin D.* Modeling extreme waves based on equations of potential flow with a free surface // J. Comp. Phys.– 2005.– 210.– P.247-273.
20. *Donelan M.A., Babanin A.V., Young I.R., Banner M.L.* Wave follower field measurements of the wind input spectral function. Part II. Parameterization of the wind input // J. Phys. Oceanogr.– 2006.– 36.– P.1672-1688.
21. *Bortkovskii R.S.* On the influence of water temperature on the ocean-surface state and transfer processes // Izv. Akad. Nauk SSSR. Fizika Atmosferi i Okeana.– 1997.– 33.– P.266-273. (*in Russian, English abstract*)
22. *Obukhov A.M.* Turbulence in an atmosphere with a non- uniform temperature // Tr. Inst. Teor. Geofiz. Akad. Nauk. SSSR.– 1946.– 1.– P.95-115.
23. *Monin A.S., Obukhov A.M.* Osnovnye zakonomernosti turbulentnogo peremeshivaniya v prizemnom sloye atmosfery // Tr. Inst. Teor. Geofiz. Akad. Nauk. SSSR.– 1954.– 24.– P.163-187. (*in Russian*)
24. *Donelan M.A., Drennan W.M., Katsaros K.B.* The air-sea momentum flux in conditions of wind sea and swell // J. Phys. Oceanogr.– 1997.– 27.– P.2087-2099.
25. *Larsen X.G., Makin V.K., Smedman A.-S.* Impact of the waves on sea drag: measurements in the Baltic Sea and a model interpretation // Glob. Atm. Oc. System.– 2003.– 9.– P.97-120.
26. *Nikolaeva Y.I., Tsimring L.S.* Kinetic model of the wind generation of waves by a turbulent wind // Izv. Atmos. Oceanic Phys.– 1986.– 22.– P.102-107.
27. *Ting C.-H., Babanin A.V., Chalikov D., Hsu T.-W.* Dependence of drag coefficient on agular spreading of sea waves // Proc. 32nd Taiwan Ocean Eng. Conf. (Taiwan, November, 2010).– 2010.– P.6.
28. *Soloviev Y.P., Kudryavtsev V.N.* Wind-speed undulations over swell: field experiment and interpretation // Boundary-Layer Meteorol.– 2010.– 136.– doi:10.1007/s10546-010-9506-z.– 23 p.
29. *Dobson F., Perrie W., Toulany B.* On the deep-water fetch laws for wind-generated surface gravity waves // Atmos.-Ocean.– 1989.– 27.– P.210-236.
30. *Badulin S.I., Babanin A.V., Zakharov V.E., Resio D.* Weakly turbulent laws of wind-wave growth // J. Fluid Mech.– 2007.– 591.– P.339-378.
31. *Gagnaire-Renou E., Benoit M., Badulin S.I.* On weakly turbulent scaling of wind sea in simulations of fetch limited growth // J. Fluid Mech.– 2010. (*in press*)
32. *Hasselmnn K., Ross D.B., Muller P., Sell W.* A paramteric wave prediction model // J. Phys. Oceanogr.– 1976.– 6.– P.200-228.
33. *Toba Y.* Local balance in the air-sea boundary processes. I. On the growth process of wind waves // J. Oceanogr. Soc. Japan.– 1972.– 28.– P.109-121.
34. *Zakharov V.E., Zaslavsky M.M.* Dependence of wave parameters on the wind velocity, duration of its action and fetch in the weak-turbulence theory of water waves // Izv. Atmos. Oceanic Phys.– 1983.– 19.– P.300-306.
35. *Davidan I.N.* Investigation of wave probability structure on field data // Tr. GOIN.– 1980.– 151.– P.8-26. (*in Russian*)
36. *Yefimov V.V., Krivinskii B.B., Soloviev Y.P.* Study of the energetic sea wind waves dependence // Meteor. Gidrol.– 1986.– 11.– P.68-75.
37. *Babanin A.V.* Spectral characteristics of surface wind wave fields: PhD Thesis.– Sebastopol, Marine Hydrophysical Institute.– 1990.– 153 p.

38. *Babanin A.V., Soloviev Y.P.* Parameterization of width of directional energy distributions of wind-generated waves at limited fetches // Izv. Atmos. Oceanic Phys.– 1987.– 23.– P.645-651.

39. *Babanin A.V., Soloviev Y.P.* Variability of directional spectra of wind-generated waves, studied by means of wave staff arrays // Marine & Freshwater Res.– 1998.– 49.– P.89-101.

40. *Babanin A.V.* Connection of parameters of the wind surface current with the wind in the north-west part of the Black Sea // Marine Hydrophysical J.– 1988.– 4.– P.55-58.

41. *Yefimov V.V., Babanin A.V.* Nonlinear effects in the wind wave spectrum // Izv. Atmos. Oceanic Phys.– 1990.– 26.– P.133-138.

42. *Babanin A.V., Polnikov V.G.* On the non-Gaussian nature of wind waves // Phys. Oceanogr.– 1995.– 6.– P.241-245.

43. *Yefimov V.V., Babanin A.V.* Dispersive relations of enevelopes of wind wave groups // Izv. Atmos. Oceanic Phys.– 1991.– 27.– P.599-603.

44. *Babanin A.V.* Field and laboratory observations of wind wave breaking / Ed. By E.Ozhan. Proc. 2nd Int. Conf. Mediterranean Coast. Env. (Tarragona, Spain, 1995).– 1995.– 3.– P.1919-1928.

45. *Banner M.L., Babanin A.V., Young I.R.* Breaking probability for dominant waves on the sea surface // J. Phys. Oceanogr.– 2000.– 30.– P.3145-3160.

46. *Babanin A.V., Young I.R.* Breaking probabilities for dominant surface waves on water of finite constant depth // J. Geophys. Res.– 2001.– C106.– P.11569-11676.

47. *Liu P.C., Babanin A.V.* Using wavelet spectrum analysis to resolve breaking events in the wind wave time series // Annales Geophysicae.– 2004.– 22.– P.3335-3345.

48. *Filipot J.-F., Ardhuin F., Babanin A.V.* A unified deep-to-shallow-water spectral wave-breaking dissipation formulation // J. Geophys. Res.– 2010.– C115.– C04022, doi:10.1029/2009JC005448.– 15 p.

49. *Evans K.C., Kibblewhite A.C.* An examination of fetch-limited wave growth off the west coast of New Zealand by a comparison with the JONSWAP results // J. Phys. Oceanog.– 1990.– 20.– P.1278-1296.

50. *Bandou T., Mitsuyasu H., Kusaba T.* An experimental study of wind waves and low frequency oscillations of water surface // Rep. Res. Inst. Appl. Mech.– 1986.– XXXIII.– P.13-32.

51. *Phillips O.M.* The equilibrium range in the spectrum of wind generated waves // J. Fluid Mech.– 1958.– 4.– P.426-434.

52. *Neumann J.* Zur Charakteristik des Seeganges // Arch. Meteorol. Geophys. Biokl.– 1954.– A7.– P.352. (*in German*)

53. *Burling R.W.* Wind generation of waves on water: PhD Dissertation.– Imperial College, University of London, 1955.– P.71-202.

54. *Bretschneide C.L.* Revisions in wave forecasting: Tech. Mem. Beach Erosion Bd.– Washington, 1958.

55. *Babanin A.V., Chalikov D., Young I.R., Savelyev I.* Predicting the breaking onset of surface water waves // Geophys. Res. Lett.– 2007.– 34.– L07605, doi:10.1029/ 2006GL029135.– 6 p.

56. *Babanin A.V., Chalikov D., Young I.R., Savelyev I.* Numerical and laboratory investigation of breaking of steep two-dimensional waves in deep water // J. Fluid Mech.– 2010.– 644.– P.433-463.

57. *Phillips O.M.* The dynamics of the upper ocean.– Cambr. Univers. Press, 1977.– 336 p.

58. *Babanin A.V., Young I.R.* Two-phase behaviour of the spectral dissipation of wind waves / Eds. By B.Edge, J.C.Santas. Proc. Ocean Waves Measurement and Analysis, 5th Int. Symp. WAVES2005 (Madrid, Spain, 3-7 July, 2005).– 2005.– № 51.– 11 p.
59. *Manasseh R., Babanin A.V., Forbes C., Rickards K., Bobevski I., Ooi A.* Passive acoustic determination of wave-breaking events and their severity across the spectrum // J. Atmos. Ocean. Technol.– 2006.– 23.– P.599-618.
60. *Toba Y.* Local balance in the air-sea boundary processes on the spectrum of wind waves // J. Oceanogr. Soc. Jpn.– 1973.– 29.– P.209-220.
61. *Zakharov V.E., Filonenko N.N.* The energy spectrum for stochastic oscillation of a fluid's surface // Dokl. Acad. Nauk SSSR (Transactions of USSR Academy of Sciences - English Translation).– 1966.– 170.– P.1992-1995.
62. *Resio D.T., Long C.E., Vincent C.L.* Equilibrium-range constant in wind-generated wave spectra // J. Geophys. Res.– 2004.– C109.– C01018, doi:10.1029/2003JC001788.– 14 p.
63. *Forristall G.Z.* Measurements of a saturation range in ocean wave spectra // J. Geophys. Res.– 1981.– 86.– P.8075-8084.
64. *Tsagareli K.N., Babanin A.V., Walker D.J., Young I.R.* Numerical investigation of spectral evolution of wind waves. 1. Wind input source function // J. Phys. Oceanogr.– 2010.– 44.– P.656-666.
65. *Babanin A.V., Tsagareli K.N., Young I.R., Walker D.J.* Numerical investigation of spectral evolution of wind waves. 2. Dissipation function and evolution tests // J. Phys. Oceanogr.– 2010.– 44.– P.667-683.
66. *Babanin A.V., Waseda T., Kinoshita T., Toffoli A.* Wave breaking in directional fields // J. Phys. Oceanogr.– 2010. (*in press*)
67. *Young I.R., Babanin A.V.* Spectral distribution of energy dissipation of wind-generated waves due to dominant wave breaking // J. Phys. Oceanogr.– 2006.– 36.– P.376-394.
68. *Willemsen J.F.* Deterministic modeling of driving and dissipation for ocean surface gravity waves in two horizontal dimensions // J. Geophys. Res.– 2002.– C107.– C83121, doi:10.1029/2001JC001029.– 17 p.
69. *Pierson W.J., Donelan M.A., Hui W.H.* Linear and nonlinear propagation of water wave groups // J. Geophys. Res.– 1992.– C97.– P.5607-5621.
70. *Hwang P.A.* Spectral signature of wave breaking in surface wave components of intermediate-length scale // J. Mar. Sys.– 2007.– 66.– P.28-37.

Материал поступил в редакцию 21.10.2010 г.